NAVAL POSTGRADUATE SCHOOL

MONTEREY, CALIFORNIA

THESIS

DIURNAL SEA BREEZE-DRIVEN CROSS-SHORE EXCHANGE ON THE INNER SHELF IN CENTRAL MONTEREY BAY

by

John E. Hendrickson

March 2009

Thesis Advisor:	Jamie MacMahan
Co-Advisor:	Karl Pfeiffer

Approved for public release; distribution is unlimited

THIS PAGE INTENTIONALLY LEFT BLANK

REPORT DOCUMENTATION PAGE			Form Approved OMB No. 0704-0188
Public reporting burden for this collection of information is estimated to average 1 hour per response, including the time for reviewing instruction, searching existing data sources, gathering and maintaining the data needed, and completing and reviewing the collection of information. Send comments regarding this burden estimate or any other aspect of this collection of information, including suggestions for reducing this burden, to Washington headquarters Services, Directorate for Information Operations and Reports, 1215 Jefferson Davis Highway, Suite 1204, Arlington, VA 22202-4302, and to the Office of Management and Budget, Paperwork Reduction Project (0704-0188) Washington DC 20503.			
1. AGENCY USE ONLY ***(Leave blank)***	**2. REPORT DATE** March 2009	**3. REPORT TYPE AND DATES COVERED** Master's Thesis	
4. TITLE AND SUBTITLE Diurnal Sea Breeze-Driven Cross-Shore Exchange on the Inner Shelf in Central Monterey Bay		**5. FUNDING NUMBERS**	
6. AUTHOR(S) John E Hendrickson			
7. PERFORMING ORGANIZATION NAME(S) AND ADDRESS(ES) Naval Postgraduate School Monterey, CA 93943-5000		**8. PERFORMING ORGANIZATION REPORT NUMBER**	
9. SPONSORING /MONITORING AGENCY NAME(S) AND ADDRESS(ES) N/A		**10. SPONSORING/MONITORING AGENCY REPORT NUMBER**	
11. SUPPLEMENTARY NOTES The views expressed in this thesis are those of the author and do not reflect the official policy or position of the Department of Defense or the U.S. Government.			
12a. DISTRIBUTION / AVAILABILITY STATEMENT Approved for public release; distribution is unlimited		**12b. DISTRIBUTION CODE**	

13. ABSTRACT (maximum 200 words)

Cross-shore exchange on the inner shelf has important impacts on the ecosystem, transporting heat, nutrients, pollutants and phytoplankton between the midshelf and surf zone. The effects of a strong (cross-shore wind stress, τ_{sx} >0.05Pa) diurnal (7-25 hrs) sea breeze on cross-shore exchange at Marina, Monterey Bay, California is investigated using two years of continuous winds, waves, and ocean velocities. Surface wind stress has spectral peaks at 1, 2, and 3 cpd and the diurnal wind variability is greater than 50%. Similar spectral energetic peaks also occur with waves and currents. During sea breeze relaxation (-0.05Pa< τ_{sx}<0.05Pa), a background wave-driven inner-shelf undertow profile exists, which is equal and opposite to Lagrangian Stokes drift, resulting in a net zero Lagrangian transport at depth. In the presence of a sea breeze (τ_{sx} >0.05Pa), a uniform offshore profile develops that is different from the background undertow profile allowing cross-shore Lagrangian transport to develop, when including Lagrangian Stokes drift. The seasonality of waves and winds modify the diurnal sea breeze impact. Therefore, material is hypothesized to incrementally move onshore near the surface and offshore near the sea bed only during sea breeze events.

14. SUBJECT TERMS Sea breeze, inner shelf, cross-shelf transport, Monterey Bay			**15. NUMBER OF PAGES** 59
			16. PRICE CODE
17. SECURITY CLASSIFICATION OF REPORT Unclassified	**18. SECURITY CLASSIFICATION OF THIS PAGE** Unclassified	**19. SECURITY CLASSIFICATION OF ABSTRACT** Unclassified	**20. LIMITATION OF ABSTRACT** UU

NSN 7540-01-280-5500 Standard Form 298 (Rev. 8-98)
Prescribed by ANSI Std. Z39.18

THIS PAGE INTENTIONALLY LEFT BLANK

Approved for public release; distribution is unlimited

DIURNAL SEA BREEZE-DRIVEN CROSS-SHORE EXCHANGE ON THE INNER SHELF IN CENTRAL MONTEREY BAY

John E. Hendrickson
Lieutenant Commander, United States Navy
B.S., North Carolina State University, 1998

Submitted in partial fulfillment of the
requirements for the degree of

MASTER OF SCIENCE IN METEOROLOGY

and

MASTER OF SCIENCE IN PHYSICAL OCEANOGRAPHY

from the

NAVAL POSTGRADUATE SCHOOL
March 2009

Author: John E. Hendrickson

Approved by: Jamie MacMahan
Thesis Advisor

Karl Pfeiffer
Co-Advisor

Jeffrey D. Paduan
Chairman, Department of Oceanography

Phillip A. Durkee
Chairman, Department of Meteorology

THIS PAGE INTENTIONALLY LEFT BLANK

ABSTRACT

Cross-shore exchange on the inner shelf has important impacts on the ecosystem, transporting heat, nutrients, pollutants and phytoplankton between the midshelf and surf zone. The effects of a strong (cross-shore wind stress, τ_{sx} >0.05Pa) diurnal (7-25 hrs) sea breeze on cross-shore exchange at Marina, Monterey Bay, California is investigated using two years of continuous winds, waves, and ocean velocities. Surface wind stress has spectral peaks at 1, 2, and 3 cpd and the diurnal wind variability is greater than 50%. Similar spectral energetic peaks also occur with waves and currents. During sea breeze relaxation (-0.05Pa $<\tau_{sx}<$0.05Pa), a background wave-driven inner-shelf undertow profile exists, which is equal and opposite to Lagrangian Stokes drift, resulting in a net zero Lagrangian transport at depth. In the presence of a sea breeze (τ_{sx} >0.05Pa), a uniform offshore profile develops that is different from the background undertow profile allowing cross-shore Lagrangian transport to develop, while including Lagrangian Stokes drift. The seasonality of waves and winds modify the diurnal sea breeze impact. Therefore, material is hypothesized to incrementally move onshore near the surface and offshore near the sea bed only during sea breeze events.

THIS PAGE INTENTIONALLY LEFT BLANK

TABLE OF CONTENTS

THIS PAGE INTENTIONALLY LEFT BLANK

LIST OF FIGURES

LIST OF TABLES

THIS PAGE INTENTIONALLY LEFT BLANK

ACKNOWLEDGMENTS

I would like to express my gratitude to Professor Jamie MacMahan for his inspiration, patience, and wealth of knowledge. He constantly challenged me as well as himself as we ventured along this journey together. I started this process as a student and eventually came out the other end (no pun intended) as a scientist. You have made this an experience that I will not soon forget.

I would also like to thank Mike Cook for the countless hours of time he spent assisting me with more MATLAB code than I ever wanted to see. To LtCol Pfeiffer, thank you for always being a wise sounding board and for reminding us all to have fun AND to not lose sight on what's really important. I would also like to acknowledge several professors at NPS that I have found to be inspiring researchers and instructors: Timour Radko, Pat Harr, Ching-Sang Chiu, Jeff Paduan and Phillip Durkee. Thank you for your hard work and dedication to your craft. It does not go unnoticed.

To my fellow section mates, we finally made it. It has been a pleasure working with and getting to know all of you. Best of luck in your future endeavors!

Finally, I would like to thank my wife Heather for her dedication and understanding. For all the times I got out of bed in the middle of the night because I just figured out what was wrong with my MATLAB code or when I would pretend to listen when I was actually thinking about a sticking point in the research or when I was just being grumpy, I thank you.

THIS PAGE INTENTIONALLY LEFT BLANK

I. INTRODUCTION

Cross-shore transport plays a significant role in the allocation and redistribution of phytoplankton, nutrients, sediment and pollutants across the continental shelf and the surf zone. Continental shelf ecosystems are some of the most dynamic on earth (Falkowski et al. 1998). Near the continental shelf break, upwelling forces nutrient-rich water to the surface causing high biological productivity, which is then transported across the continental shelf (Pilskaln et al. 1996). Therefore, it is important to understand the mechanisms responsible for cross-shore exchange. There are three primary regions located shoreward of the outer continental shelf, which are referred to as the midshelf, inner-shelf and surf zone, and are dominated by different dynamics (Lentz 1999).

For the midshelf, cross-shore transport is the result of steady alongshore wind stresses acting together with the Coriolis force producing a transport of water at a right angle to the predominant wind direction in the Northern Hemisphere, known as Ekman transport (Ekman 1905, Sverdrup 1938, Csanady 1978, Lentz 1992, Dever 1997a). On the midshelf, during upwelling or downwelling events, the midwater pycnocline intersects the surface or bottom boundary, forming a front that moves offshore. During both upwelling and downwelling, full Ekman transport develops in the midshelf region because the strong stratification of the pycnocline acts to insulate the surface and bottom layers from each other (Austin and Lentz 2002). The region seaward of this dynamic front is the midshelf and the region shoreward of the front is the inner-shelf (Lentz 1994, Austin and Lentz 2002).

On the inner shelf, as the water depth decreases, the alongshore surface stress becomes increasingly balanced by the bottom stress instead of the Coriolis force, reducing Ekman surface boundary layer transport (Dever et al. 2006). Numerical model studies (Austin and Lentz 2002, Tilburg 2003) and observations on the inner-shelf regions of North Carolina (Lentz 1999, 2001),

Massachusetts (Fewings et al. 2008), Oregon (Kirincich et al. 2005) and California (Cudaback et al. 2005) found that alongshore winds are not a sufficient mechanism in driving cross-shore circulation on the inner-shelf. Tilburg (2003) numerically found that cross-shore winds induced a two-layer circulation consisting of onshore transport near the sea surface and an equal and opposite offshore transport below that allowed for cross-shore exchange.

The surf zone is defined as the region between depth-limited breaking (Thornton and Guza, 1983) and the shoreline. The mechanisms for cross-shore transport in the surf zone are wave-driven and consist of Stokes drift, undertow, and rip currents. Stokes drift is the time-averaged second order velocity of a fluid particle under a wave. There is an incomplete closure of the parcel path after each wave period resulting in a net drift in the direction of wave propagation (Stokes 1847, Madsen 1978). The associated mass transport occurs between the wave trough and crest in the Eulerian frame and is vertically distributed below mean sea level (MSL) in the Lagrangian frame. The theoretical cross-shore Stokes transport, Q_{stokes} is,

$$Q_{stokes} = \frac{gH_{sig}^2}{16c}\cos\theta_w \quad (1)$$

where g is the gravitational acceleration, H_{sig} is the significant wave height, c is the phase speed of the waves, and θ_w is the wave direction relative to shore normal (Stokes 1847, Longuet-Higgins 1953). The onshore transport near the surface is balanced by an equal transport in the opposite direction at depth, the undertow (Ursell 1950, Haines and Sallenger 1994, Reniers et al. 2004). In the surf zone, the compensating return 2D vertical profile is parabolic with a maximum offshore flow at mid-depth and close to wave breaking.

Undertow affects the 2D vertical profile, while rip channels affect the 2D horizontal circulation (assuming the vertical is depth-uniform) allowing for transport of material across the surf zone. Alongshore bathymetric variations create alongshore variations in depth-limited wave breaking that induce

alongshore gradients in pressure and momentum driving water from the shore-connected shoals toward rip channels (Bowen 1969, Dalrymple 1978). Onshore flows over the shore-connected shoals or bars transition to alongshore flows (feeder currents) near the shoreline that converge in the rip channel and extend seaward across the surf zone, and beyond (Shepard et al. 1941, Inman and Brush 1973). Inman and Brush (1973) referred to rip currents as “freeways” that transport material outside the surf zone to the inner-shelf.

A. MECHANISMS FOR CROSS-SHORE TRANSPORT ON THE INNER-SHELF

Hasselmann (1970) suggested that the Coriolis force acting on the surface wave flow induces a small along-crest wave velocity that is in phase with the vertical wave velocity resulting in a “wave stress”. Xu and Bowen (1994) theoretically determined that the “Hasselmann” wave stress is balanced by the Coriolis force in the alongshore momentum balance, resulting in an offshore-directed Eulerian flow, which is equal and opposite to the Lagrangian Stokes drift, resulting in a zero net transport over the vertical as suggested by Ursell (1950). This would explain why the ocean does not pile up with water at the shoreline owing to the shoreward transport of Stokes drift. The presence of this compensating offshore-directed Eulerian flow has been observed outside of the surf zone in the field (Reniers et al. 2004, Smith 2006, Lentz et al. 2008) and in laboratory studies (Putrevu and Svendsen 1993, Ting and Kirby 1994, Cox and Kobayashi 1997, Monosmith et al. 2007).

Lentz et al. (2008) compared the wave-driven velocity profiles from Martha’s Vineyard Coastal Observatory, MVCO, to the theoretical work by Xu and Bowen (1994). The model by Lentz et al. (2008) assumes steady-state, linear dynamics with alongshore homogenous variations, and constant density. The model is based on the continuity and momentum balances,

$$\int_{-h}^{0} u\, dz = -Q_{stokes}\,, \tag{2}$$

$$-fv = fv_{st} - g\eta_x - F^{ws} + \tau_z^{wbx}/\rho_o + (Au_z)_z , \quad (3)$$

$$fu = -fu_{st} + \tau_z^{wby}/\rho_o + (Av_z)_z , \quad (4)$$

where Q_{stokes} is the onshore Stokes transport, fv and fu are the Coriolis forces, fv_{st} and fu_{st} are the Hasselmann wave stresses, g is gravitational acceleration, η_x is the cross-shelf pressure gradient, F^{ws} is momentum flux divergence, τ_z^{wbx}/ρ_o and τ_z^{wby}/ρ_o are the near bottom wave stresses, $(Au_z)_z$ and $(Av_z)_z$ are the turbulent eddy viscosities (see Lentz et al. (2008) for a detailed description of the model). For small eddy viscosities (indicative of motions outside the surf zone) the offshore velocity profiles had a curvature with a maximum offshore flow near the surface, that decreases with decreasing depth. These modeled profiles favorably matched the field observations at MVCO outside the surf zone. In the absence of wind, Lentz et al. (2008) concluded that the time-averaged flow in the inner shelf is primarily associated with undertow that is driven by surface gravity waves and influenced by the Hasselmann wave stress.

Prior to the work of Tilburg (2003), cross-shelf winds were considered ineffective in forcing cross-shelf transport due to the cross-shelf components of the surface and bottom boundary stress being an order of magnitude smaller than the Coriolis force of the alongshelf flow (Csanady 1978; Allen 1980). Fewings et al. (2008) observed that the cross-shore wind forcing was important for cross-shelf exchange, as it modifies the wave driven undertow profile found by Lentz et al. (2008), inducing a two-layer flow circulation. The surface flow below the wave trough was in the direction of wind forcing, consistent with previous estimates of surface wind-induced drift (Wu, 1983, Ogasawara and Yasuda 2004), and a compensating return flow in the bottom portion of the profile was in the opposite direction of the wind forcing. The presence of a cross-shore wind results in a non-zero net transport at depth. Fewings et al. (2008) found that as background wave forcing increased, the two-layer circulation resulting from wind forcing was subjugated by the wave-driven undertow, which is always directed offshore. When wave and wind forcing were in the same direction, the

cross-shelf velocity profile is practically vertically uniform owing to the vertical shears being similar in magnitude but opposite in direction. When wind and wave forcing were in opposing directions, the cross-shelf velocity profile is strongly sheared owing to the vertical shears being large and in the same direction.

The Lagrangian velocity, u_L, is defined as,

$$u_L = u_E + u_s \tag{5}$$

where u_E is Eulerian velocity and u_S is Stokes drift velocity. For the wave-driven undertow on the inner-shelf, u_E and u_S are equal and opposite at depth resulting in zero u_L at depth (Xu and Bowen, 1994; Lentz et al. 2008). This results in zero net transport. However, when the undertow profile is modified due to winds (Fewings et al. 2008), the transport is onshore (offshore) near the surface and offshore (onshore) near the sea bed with onshore (offshore) winds, with the depth-integrated transport equal to zero.

Lentz et al. (2008) confirmed that the forcing mechanisms for cross-shelf exchange on the inner shelf are fundamentally different from those at midshelf. Fewings et al. (2008) evaluated the relative importance of cross- and alongshore wind and wave forcing as a function of water depth and suggested that cross-shore wind stress is the primary forcing mechanism for cross-shelf exchange for water depths less than 30 m.

B. SEA BREEZE

The diurnal sea breeze is the result of a difference in air pressure between the land and ocean caused by differential heating, which occurs for approximately two-thirds of the earth's coasts (Defant 1951, Atkinson 1981, Simpson 1994). Owing to a difference in thermal heat capacity, the land heats and cools more rapidly than the ocean, generating an intense onshore sea breeze in the late afternoon and a weaker offshore land breeze during the night (Defant 1951, Atkinson 1981, Simpson 1994).

Woodson et al. (2007) observed that the diurnal sea breeze in northern Monterey Bay was responsible for local upwelling resulting in offshore Ekman transport during the day. The sea breeze at this site is predominantly parallel to the shoreline (Figure 1). Note that our study site is located in the center of Monterey Bay and focuses on similar events (Figure 1), where the winds are predominantly perpendicular to the shoreline. Woodson et al. (2007) suggests that this local diurnal upwelling may supply nutrients to nearshore kelp beds and transport larvae to nearshore habitats.

The effects of a diurnal sea breeze and waves on cross-shelf exchange on the inner shelf are examined at Marina, Monterey Bay, CA. It is hypothesized that the sea breeze diurnally modifies the vertical current profile allowing for cross-shore exchange to develop. Two years of continuous ocean velocity, wave, and wind data are analyzed and described below for testing the proposed hypothesis.

II. OBSERVATIONS

The subaqueous ocean velocity profiles, with a bin size of 0.5 m, and co-located pressure were measured continuously at 1 Hz by a bottom-mounted 1200-kHz broadband Acoustic Doppler Current Profiler (ADCP) deployed in approximately 13 m water depth at 36°42.0'N, 121°48.9'W (Figure 1) from 01 January 2006 to 31 December 2008. Surface winds and air temperature were measured every 2 minutes by a wind anemometer mounted on a 10 m tripod on a local sand dune that was 51 m above sea level and approximately 2.5 km east of the ADCP site at Marina Airport (36°40.9'N, 121°46.0'W) (Figure 1). Daily records with greater than 30 percent erroneous or missing data were not considered in the analyses. The remaining data were quality-controlled by applying a 3-standard deviation filter to remove outliers (Emory and Thomson, 2001).

Since it is difficult to recognize the sea surface with ADCP velocity observations, sea surface elevations were estimated by transforming the co-located ADCP pressure measurements applying linear wave theory. Previous studies have not used the ADCP velocity measurements above the wave trough due to acoustic surface reflections (Fewings et al. 2008, Lentz et al. 2008) and difficulties identifying the sea surface. Instead, wave-driven surface transport (Stokes drift) is estimated using linear wave theory. The variability of surface transport by waves and winds is an important aspect of this research, so ADCP velocities above the trough are included. ADCP velocities above the calculated sea surface elevation were set to zero. The 1 Hz velocity profile was depth-normalized by using a low-pass filtered (f<0.04Hz) sea surface elevation, which includes infragravity waves (Herbers et al. 1994) and tides. This allows the high-frequency waves (f>0.04 Hz) associated with sea and swell waves to fluctuate around z/h=1, referred to as mean sea level (MSL). The depth normalization also removes the tidal modulation allowing the time records greater than 3 hours to be compared. The normalized scale was set from z/h = 0 at the sea bed to z/h = 1.5

at the highest wave crest with 0.05 vertical increments. For the purposes of calculating transport, the flow was considered vertically uniform between the first good bottom bin (z/h = 0.2) and the sea bed.

Cross-shore velocity magnitudes are easily affected by slight rotational errors in the local coordinate frame due to the tidal currents being predominantly alongshore (Rosenfeld et al. 2008). A Principal Component Analysis (PCA) was used to determine the local coordinate frame orientation (Figure 2), where the alongshore velocity component is defined as the major axis of the subtidal depth-averaged velocity, $\boldsymbol{u}_{da}$, computed from zero depth-crossing to the sea bed (Davis, 1986). For quality control purposes, the PCA was estimated for all normalize depths to prevent biases associated with surface gravity waves and bottom drag owing to to bed stress. It was found that between z/h = 0.25 and z/h = 0.75, the PCA's were within 1°. Below z/h = 0.25 and above z/h = 0.75 the PCA rotational angles were inconsistent. The final PCA used a $\boldsymbol{u}_{da}$ between the depths of z/h = 0.25 and z/h = 0.75 indicating that the major principal axis was oriented 10° clockwise from true north, consistent with local isobaths from a recent nautical chart (Monterey Bay 18685 33rd edition September 2005) (Figure 1). A right-handed coordinate system is used, where x is positive cross-shore eastward, y is positive alongshore northward, and z is positive upward.

At this location, the winds are predominantly cross-shore making it an ideal location for studying cross-shore sea breezes effects. Surface wind stresses (τ_s) were calculated using the model from STRESSTC (Smith 1988) using wind speed and air temperature at a height of 10 m above ground. Cross-shore surface wind stress (τ_{sx}) and along-shelf surface wind stress (τ_{sy}) were rotated to the same local coordinate system defined by $\boldsymbol{u}_{da}$. The local wind stress rose histogram indicates that 90% of the stresses resided between +/- 20 degrees of shore-normal with a mean of 0.074 Pa and variance of 0.024 Pa^2 (Figure 3). The mean wind direction is + 6 degrees relative to shore-normal. The diurnal τ_{sx} is skewed (skewness=1.61) onshore. τ_{sx} has intense onshore stress that last for a short duration followed by a longer minimal offshore stress. Unlike

the MVCO field site (Fewings et al. 2008), Monterey Bay has a strong and consistent year round diurnal sea breeze (Figure 4).

The inner shelf was previously defined as the region inshore of the upwelling and downwelling front where the surface and bottom Ekman layers interact (Lentz 1994, Austin And Lentz 2002, Tilburg 2003). Tilburg (2003) uses the formula presented in Weatherly and Martin (1978) to determine whether the site is located in the midshelf or the inner shelf,

$$\delta = C_1 \sqrt{\frac{\tau_s}{\rho}} \frac{1}{f(1+\frac{N^2}{f^2})^{\frac{1}{4}}} \tag{6}$$

where C_1 is a fitting parameter and is estimated by Tilburg to be 2.3, f is the Coriolis parameter and N is the buoyancy frequency. When δ is greater than the local water depth (*h*), the region is considered to be the inner shelf. The average value for N in Monterey Bay is 3.5 x 10^{-3} s^{-1} with an f = 8.7 x 10^{-5} s^{-1} (Petruncio et al. 1998, Rosenfeld et al. 1994). At the measurement site in Monterey Bay τ_s ≥ 0.005 Pa 99% of the time resulting in δ greater than *h* suggesting this site is always in the inner shelf. Though stratification may be important at different times of the year, it is assumed small for this analysis.

THIS PAGE INTENTIONALLY LEFT BLANK

III. RESULTS

A. SPECTRAL ANALYSIS

Record composed of 20-minute block averaged values over 730 days. Spectra were calculated using a Hanning window with 50% overlap resulting in 102 degrees of freedom and frequency resolution of 0.003 cycles per hour (cph). Spectra are examined in the diurnal frequency band (0.03-0.13 cph). Energetic spectral peaks for wind stresses and waves occur at diurnal, 1 cycle per day (cpd) (f = 0.042 cph), 2 cpd, semi-diurnal, (f = 0.083 cph) and 3 cpd (f = 0.125 cph) (Figure 5). The energy at 1 cpd peak is the greatest and is three times larger than at 2 cpd and ten times larger than at 3 cpd, where the 2 and 3 cpd peaks are the wind harmonics. Velocity spectra were estimated at each elevation and vertically stacked. The 2-D cross-shore velocity spectra indicates a significant diurnal peak throughout most of the column and less energetic peaks near the surface at 2 and 3 cpd (Figure 5). The 2-D alongshore velocity spectra are an order of magnitude greater than in the cross-shore and have broader energy at 1 and 2 cpd that occur throughout the column. The energetic spectral peaks are associated with tidal constituents (i.e., S1, K1, M2, S2, and S4) and the diurnal wind harmonics (Militello and Kraus 2001). There is a significant coherence at the 95% level between the cross-shore wind and the cross-shore velocity at 1, 2, and 3 cpd (not shown). There is no significant coherence between the cross-shore winds and the alongshore velocities for the same frequencies (not shown). In order to resolve the K1 and 1 cpd spectral energy peaks, a maximum frequency resolution, Δf, must be defined,

$$\Delta f = \frac{f_{K_1} - f_{S_1}}{4} = \frac{\frac{1}{23.93\ hr} - \frac{1}{24\ hr}}{4} = 1367\ days. \quad (7)$$

The window length is 1/Δf. For this example, a minimum of 1367 days (3.75 years) is required, while only providing 2 DOF. The observations described

herein for 2 years shorter than the 3.75-year requirement. Therefore, spectral analysis is unable to resolve these peaks.

B. DIURNAL VARIABILITY

Diurnal variability is defined as the variance of the high-pass (<25hrs) filtered signal divided by the variance of the total signal. The cross-shore sea breeze represents over 56% of the total surface wind variability (Table 1). The diurnal variability of waves is about 20%, which is influenced by the diurnal sea breeze. The diurnal variability of the surface velocities (z/h = 1) is 24% in the cross-shore and 28% in the alongshore, whereas below the trough, the $\boldsymbol{u}_{da}$ diurnal variability is 62% in the cross-shore and 32% in the alongshore.

Since many of the significant tidal constituents occur within the diurnal frequency band, tidal current variability is examined (Table 2). The tidal current variability is calculated as the variance of the predicted diurnal tidal currents found using the T_TIDE program (Pawlowicz et al. 2002), divided by the variance of the total current at each z/h. Previous studies suggest that a record of 366 or more days is needed to resolve S1 from K1 using T_TIDE (Rosenfeld et al. 2008, Petruncio et al. 1998). Variability of the calculated depth-averaged tidal velocity in the cross- and alongshore are 9% and 20% (Table 1). However, the 2 and 3 cpd sea breeze harmonics coincide with the S2 and S4 tidal constituents and cannot be separated using T_TIDE. Militello & Kraus (2001) found it difficult to differentiate diurnal tidal constituents from wind harmonics. It is assumed that the mean sea surface elevation is not influenced by the sea breeze, whereas the velocities are influenced. T_TIDE applied to the averaged sea surface elevation predicts 99.9% of the observed signal. The predicted S1, S2, and S4 combined tidal elevation represents 0.5% of the total prediction. Currently, we are unaware of any Fourier method that exists to distinguish motions at the same frequency with different phases (Appendix A). It is assumed that the velocities associated with S2 and S4 are weak, owing to the less than 0.5% surface contribution, and predominantly in the alongshore (Rosenfeld et al. 2008).

Owing to the small cross-shore velocities, a typical day is divided into 24 one-hour increments, where a mean velocity for each hour in the day is averaged over the 2 years (defined as the 24-hr time-averaged method). This approach increases our confidence in the mean hourly velocities (Bendat and Piersol 2000) that varies over the day, which is hypothesized to be related to the diurnal sea breeze. This approach retains the background flow field at this site. The confidence error ($\pm 1.65\ \sigma / \sqrt{n}$) on the mean at the 90% significance level for the subaqueous (below the wave trough) where σ is the standard deviation of the velocity are 0.001 m/s and 0.003m/s at the surface. The 24-hr time-averaged method applied to the predicted tidal cross-shore tidal velocities for the subaqueous and surface regions are 0.001 and 0.003 m/s. Therefore, the total expected error for the subaqueous and surface regions are 0.002 and 0.006m/s, where the signals are an order of magnitude greater than these errors.

THIS PAGE INTENTIONALLY LEFT BLANK

IV. DISCUSSION

A. SUBTIDAL (>25HRS) MEAN CURRENT PROFILES

Consistent with Fewings et al. (2008), the 20-minute time-averaged velocities were de-tided using T_TIDE (Pawlowicz et al. 2002) and low-pass filtered (> 25 hour) to evaluate the subtidal (>25 hrs) profile. The 2 years of cross-shore vertical velocity profiles were sub-divided into four sub-categories: when both τ_{sx} and H_{sig} are small, when either τ_{sx} or H_{sig} are large and the other small, and when both forcing mechanisms are large. A one standard deviation criteria was used to define when τ_{sx} and H_{sig} were large or small. τ_{sx} was considered small when less than 0.05 Pa and large when greater than 0.1 Pa. H_{sig} was considered small when less than 0.7 m and large when greater than 1.7 m.

When τ_{sx} and H_{sig} were small, the mean cross-shore profile had a small offshore velocity of 1.5 cm/s just below the trough that diminished to zero half way down the column (Figure 6a). This mean background cross-shelf velocity profile was subtracted from the other three mean profiles shown in Figure 6 b-d. During large τ_{sx} (when H_{sig} is weak), there is an increase in the onshore surface flow of 2 cm/s due to wind-induced drift (Figure 6b). The subaqueous flow has a two-layer structure with onshore flow of 2 cm/s in the upper portion of the water column and offshore flow of 1 cm/s in the lower portion of the column. These cross-shore results are consistent with observations at MVCO (Fewings et al. 2008), Santa Barbara Channel (Cudaback et al. 2005) and model results (Tilburg 2003). During large H_{sig} (when the τ_{sx} is weak), the surface flow increased significantly to 11 cm/s, likely due to Stokes drift (Figure 6c). The subaqueous cross-shore flow was offshore throughout the water column and intensified near the surface to 1.5 cm/s. These observations are similar to the inner-shelf undertow profile by Lentz et al. (2008). When both τ_{sx} and H_{sig} are large, the profile became more vertically uniform, consistent with Fewings et al. (2008)

results. The surface flow was onshore at 16 cm/s and below the trough the offshore flow was 2 cm/s. In summary, the subtidal cross-shore profiles at Monterey are similar to the results by Lentz et al. (2008) and Fewings et al. (2008). It is important to note that τ_{sx} >0.05 Pa is the threshold considered to modify the wave-driven undertow profile.

B. DIURNAL (7-25HRS) VARIABILITY

The thermally induced sea breeze begins to develop at 1630 GMT in the presence of near zero background τ_{sx} (Figure 7a). The τ_{sx} peaks at 2200 GMT with a magnitude 0.08 Pa, and exceeds the threshold of 0.05 Pa suggesting that it will modify the undertow profile. Since the sea breeze initiates near the shoreline, there is no immediate diurnal impact on H_{sig} due to a minimal fetch (Massel 1996). As the sea breeze develops (τ_{sx} > 0.05 Pa), its extends both landward and seaward increasing the fetch. As the fetch increases (and duration), the sea breeze begins to influence the waves at 2300 GMT and peaking at 0200 GMT with a H_{sig} of 1.4 m (Figure 7b). The sea breeze enhances H_{sig} by an average of 25 cm or 16 % of the mean H_{sig}. Surface flow is onshore throughout the day due to a combination of Stokes drift and wind-induced drift (Figure 7c). As the sun sets, the thermal gradient dissipates due to the cooling of the coastal land (Banta et al. 1993, Banta 1995). The “typical day” in Monterey indicates no offshore flow from a land breeze consistent with Banta et al. (1993) and Banta (1995). This time period of minimal diurnal forcing (-0.05 Pa < τ_{sx} < 0.05 Pa) is called the relaxation period, and is below the threshold values for wind to modify the undertow profile. Below the trough during the relaxation period, though winds and waves are present, it is considered to be wave-dominated with a maximum offshore of 3 cm/s near the surface, which is consistent with the Lentz et al. (2008). These results suggest that the undertow is always present at this site owing to the background presence of waves. Once the sea breeze develops (τ_{sx} > 0.05 Pa), the below trough profile is near vertically uniform offshore, similar to the results for combined cross-shore wind and wave

forcing found in the subtidal results (Section 4.1) and by Fewings et al. (2008). The background undertow profile is modified during the sea breeze allowing for the onshore transport near the surface and offshore transport near the sea bed, which is not reversed during relaxation.

C. SEASONAL MODULATION OF THE DIURNAL VARIABILITY

The sea breeze persists year round at Monterey Bay and only changes seasonally in intensity (Figure 4). The 24 hr time-averaged method was evaluated seasonally using the four northern hemisphere meteorological seasons, Spring (March 1st through May 31st), Summer (June 1st through August 31st), Fall (September 1st through November 30th) and Winter (December 1st through February 28th) (Trenberth, 1983). For seasonal evaluation, the subaqueous current data were high-pass filtered (<25hr) in order to enhance the diurnal variability.

The τ_{sx} and H_{sig} were separated into four seasons to examine the seasonal influence on the diurnal variability (Figure 8). The velocity data were high-pass filtered (< 25 hr) to enhance the diurnal variability amongst the seasons.. During the spring months, the thermal gradient begins to increase along the coast resulting in the strongest sea breeze. τ_{sx} has a background of 0.01 Pa and peaks at 0.11 Pa at 2300 GMT. H_{sig} increases 0.25 m to a peak of 1.55 m from a background H_{sig} of 1.2 m at 0300 GMT. In summer, thermal heating continues to drive the sea breeze with τ_{sx} background of 0.01 Pa and peaks at 0.1 Pa at 2200 GMT. Due to the eastern Pacific Ocean storm season ending, the background H_{sig} reduces to 0.9 m and diurnally peaks at 1.3 m at 0300 GMT. The summer season represents a period when diurnal winds are the most significant compared to background waves. It also has the largest effect on generating sea beeze driven waves, increasing H_{sig} by 0.4 m. In the fall, days begin to get shorter resulting in a reduced coastal thermal gradient. The background τ_{sx} is 0 Pa and peaks at 0.7 Pa at 2200 GMT. For the first time, τ_{sx} becomes slightly negative. In the fall, waves begin to be influenced by the onset

of the winter storm season with a background H_{sig} of 1.15 m to a sea breeze enhanced peak of 1.3 m at 0100 GMT. In the winter months, the thermal gradient continues to weaken, resulting in a background τ_{sx} of -0.01 Pa with a sea breeze peak of less than 0.04 Pa at 2400GMT. The background H_{sig} is the largest (~1.6 m) and no distinct peaks exists, though there is a subtle background trend, which is highest around 0100 GMT and slowly decays throughout the day. The diurnal forcing is the weakest in the winter.

Seasonal surface and subaqueous (below wave trough) cross-shore velocities (Figure 9) are examined as a function of a seasonal diurnal τ_{sx} and H_{sig} (Figure 8) The velocities in the surface region are the largest in the winter, owing to larger waves, even though τ_{sx} is the lowest at this time. The surface velocities remain large in the spring, which still have large background waves. The summer has the lowest surface velocities because this period has the smallest background waves. The surface velocities for all seasons vary diurnally. The diurnal variability is enhanced in the fall, as it a period with relatively constant H_{sig}, but strong diurnal τ_{sx} variation.

For the subaqueous region (z/h<0.75) during sea breeze events (when τ_{sx} >0.05, 2000-2400 GMT), a vertically uniform offshore profile exists. The profile velocity magnitude increases with increasing seasonal background wave height. During the locally generated sea breeze waves (0100-0600 GMT), there is minimal enhancement of the velocity profile, which increases with increasing seasonal background wave height. During the relaxation period (0800-1600 GMT), the velocity profiles have vertical variations that vary seasonally. Since the τ_{sx} only exceeds the 0.05Pa threshold during the sea breeze, the velocity profiles vary primarily as a function background waves over the seasons. The vertical profile structure is consistent with subtidal velocity structure (Section 4.1), Lentz et al. (2008), and Fewings et al. (2008).

D. CROSS-SHORE TRANSPORT

The quantitative variation of surface drift as a function of its forcing parameters remains poorly understood (Ardhuin et al. 2008, Ardhuin et al. 2004, Rascle et al. 2004). Ardhuin et al. (2004, 2008) suggest that Stokes drift due to wave forcing typically accounts for two-thirds of the surface wind-induced drift, but these estimates are not exact and require additional research. The Monterey Bay site is dominated by a year-round sea breeze leading to a significant daily wind-induced drift. The theoretical Stokes drift (Q_{stokes}) is correlated with the estimated surface transport ($Q_{surface,ADCP}$) at the 95% significance level with a slope (m) of 0.42 and a coefficient of determination (r^2) of 0.57 implying that the measured surface transport is over estimated by ~50%. A linear regression of Q_{stokes} and $Q_{surface,ADCP}$, when τ_{sx} was minimal (-0.005 Pa =< τ_{sx} <= 0.005 Pa) resulted in a m of 0.89 and a r^2 of 0.57 suggesting that the difference in the predicted and measured surface transports are related to cross-shore wind-drift, which is close to the estimates by Ardhuin et al. (2004, 2008) . The difference in the predicted and measured transports may also be related to the fact that ADCP measurements are problematic and/or the bin size is not adequate to resolve the transport in the trough-crest region. Even though potential biases exist, the observations are used to examine the diurnal surface transport within the trough-crest region.

Q_{stokes} is correlated with the estimated ADCP sub-surface depth integrated transport ($Q_{sub\text{-}surface,ADCP}$) at the 95% significance level with a m of 0.89 and an r^2 of 0.29. These results indicate a balance in transport estimates, but recognize that this relationship is weak.

When the sea breeze develops, there is an immediate increase (decrease) in $Q_{surface,ADCP}$ ($Q_{sub\text{-}surface,ADCP}$) suggesting that the winds are influencing the transport (Figure 10). When the sea breeze induced H_{sig} increase,, $Q_{surface,ADCP}$ and Q_{stokes} increases by the same magnitude while $Q_{sub\text{-}surface,ADCP}$ weakens. During the relaxation period, $Q_{surface,ADCP}$ decreases at a

greater rate than Q_{stokes}, which does not include a theoretical wind-drift. Although $Q_{surface,ADCP}$ and Q_{stokes} increase with roughly the same magnitude during the diurnal wave forcing, $Q_{surface,ADCP}$ continues to be nearly double the magnitude of Q_{stokes} during the relaxation period, which is related to the background wind-drift or ADCP errors.

Two separate net transports were calculated, where the first net transport (Q_{net1}) is the sum of $Q_{surface,ADCP}$ and $Q_{sub\text{-}surface,ADCP}$ (green triangles) resulting in net onshore of 5.2×10^{-2} m^2/s and the second net transport (Q_{net2}) is the sum of Q_{stokes} and $Q_{sub\text{-}surface,ADCP}$ (magenta triangles) resulting in net offshore of 5.3×10^{-2} m^2/s. During sea breeze, Q_{net2} (Q_{net1}) is increased (reduced) in the offshore (onshore). During relaxation, Q_{net2} is relatively balanced in the cross-shore, even when the sea breeze driven waves increases, which is consistent with the idea of zero net balance at depth (Lentz et al. 2008).

A slight rotational error in the coordinate frame of reference may be influencing Q_{net1} and Q_{net2} . As mentioned earlier, the coordinate frame orientation was based on a PCA of the $\boldsymbol{u}_{da}$ between the normalized depths of 0.25 to 0.75, which resulted in a clockwise rotation of the coordinate system by 10 degrees. A subsequent PCA of the surface flow resulted in a clockwise rotation of 16 degrees. This, along with the site's complex bathymetry due to its proximity to the Monterey Bay canyon suggest there may be a slight discrepancy in the rotation coordinate frame orientation. Simple adjustments to the rotation angle based on net transports resulted in a required clockwise rotation of 17 degrees to obtain a Q_{net1} of zero and a required clockwise rotation of 2 degrees yielding a Q_{net2} near zero. The small changes in coordinate frame rotation required to balance the net transports signify the importance of a precise coordinate frame orientation.

V. SUMMARY AND CONCLUSIONS

Two years of measured cross-shore velocity profiles, which varied as a function of wind and wave forcing were examined on the inner shelf in Monterey Bay with particular emphasis on the diurnal variability associated with sea breezes. In the absence of winds, subtidal (>25hrs) cross-shore velocity profiles consist of a wave-driven undertow profile as described by Lentz et al. (2008) and were modified in the presence of wind (Fewings et al. 2008). The diurnal (<25hrs) variability of winds, waves, and ocean currents represent approximately 50% of the total signal. On the diurnal (7-25hrs) temporal scale, the winds and waves vary diurnally with a repetitive nature. Onshore winds increasing in the afternoon for a short duration, referred to a sea breeze. During the subsequent land breeze (relaxation), the winds are reversed offshore, but because of the mean background onshore wind, a true offshore wind stress rarely occurs in Monterey, CA. The diurnal sea breeze increases the local waves with a maximum occurring a few hours after the maximum in the winds. When the sea breeze occurs, the wind stress exceeds 0.05 Pa, which is an arbitrary threshold for when the velocity profile is influenced by winds. The background velocity profile in Monterey is a wave-driven undertow profile that is only modified during sea breeze events. Results suggest wind and wave forcing have similar effects on the surface and subaqueous current structure on both the subtidal and diurnal scales. The velocity profiles vary seasonal owing to storms and difference in thermal gradients. However, a similar diurnal velocity profile trend exists with only subtle seasonal modifications associated with changing wind and wave magnitudes.

The background Eulerian wave-driven undertow is equal and opposite to the Lagrangian Stokes drift, the net transport at depth is zero resulting in no cross-shore transport. When the sea breeze occurs, τ_{sx} > 0.05 Pa, the undertow profile is modified and the net transport at the surface is shoreward and seaward near the sea bed, referred to as a two layer circulation. During the relaxation period (land breeze), the τ_{sx} is not large enough to modify the background

undertow profile or able to reverse the previous sea breeze transport. Therefore, material is hypothesized to incrementally move onshore near the surface and offshore near the sea bed only during sea breeze events, which are periodic at the center of Monterey Bay.

APPENDIX A: FOURIER ANALYSIS ON A SIGNAL COMPOSED OF TWO SINUSOIDS WITH THE SAME FREQUENCY AND DIFFERENT PHASE

If a signal, g(t), is composed of two sinusoids with the same frequency and a different phase, defined as

$$g(t) = Acos(\omega t) + Bcos(\omega t + \alpha) \quad \text{(a1)}$$

where A and B are the amplitude of the two signals, ω is the radian wave frequency, and α is the phase difference. g(t) can be re-written using a trigonometric identity,

$$g(t) = Acos(\omega t) + Bcos\,\omega t\,cos\alpha - Bsin\,\omega t\,sin\alpha \quad \text{(a2)}$$

The Fourier in-phase amplitude, a_n, is computed by,

$$a_n = \frac{2}{T}\int_0^T Acos(\omega t)cos\omega t + \frac{2}{T}\int_0^T Bcos(\omega t)cos\omega t\,cos\,\alpha - \frac{2}{T}\int_0^T Bsin\alpha\,sin\omega t\,cos\omega t \quad \text{(a3)}$$

resulting in

$$a_n = A + Bcos\alpha \quad \text{(a4)}$$

The Fourier out-of-phase component, b_n, is computed by

$$b_n = \frac{2}{T}\int_0^T Acos(\omega t)sin\omega t + \frac{2}{T}\int_0^T Bcos(\omega t)\,sin\omega t\,cos\,\alpha - \frac{2}{T}\int_0^T Bsin\alpha\,sin\omega t\,sin\omega t \quad \text{(a5)}$$

resulting in

$$b_n = Bsin\alpha \quad \text{(a6)}$$

The Fourier coefficients are composed of amplitudes from both sinusoids resulting in two equations with three unknowns, so without knowing the exact phase difference, the two signals cannot be separated.

THIS PAGE INTENTIONALLY LEFT BLANK

APPENDIX B. FIGURES AND TABLES

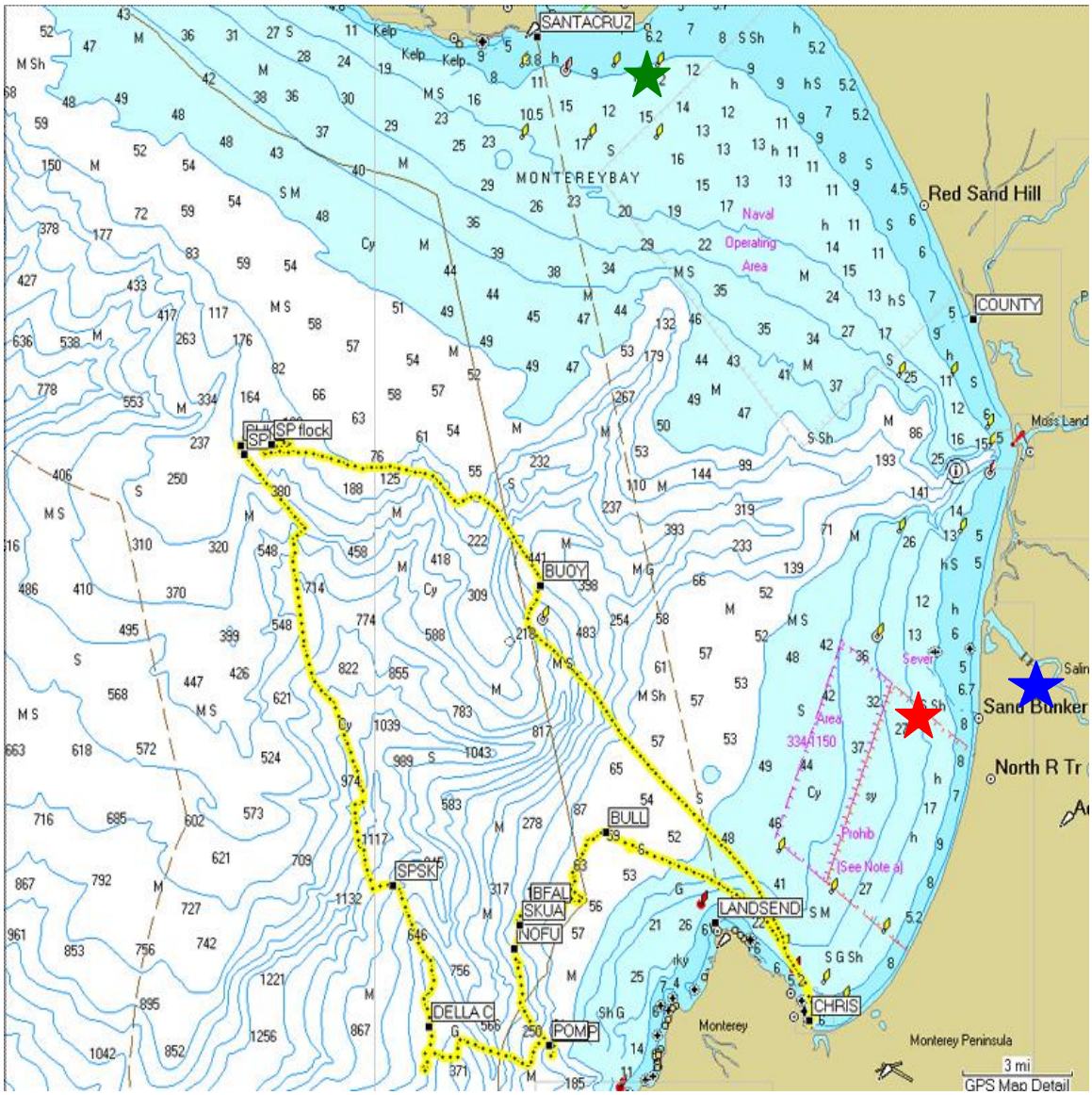

Figure 1. Bathymetry view of Monterey Bay, CA. Red star indicates the location of the ADCP in 13m water depth and the blue star indicates the location of the wind anenometer. Green star indicates site location for Woodson et al. (2007).

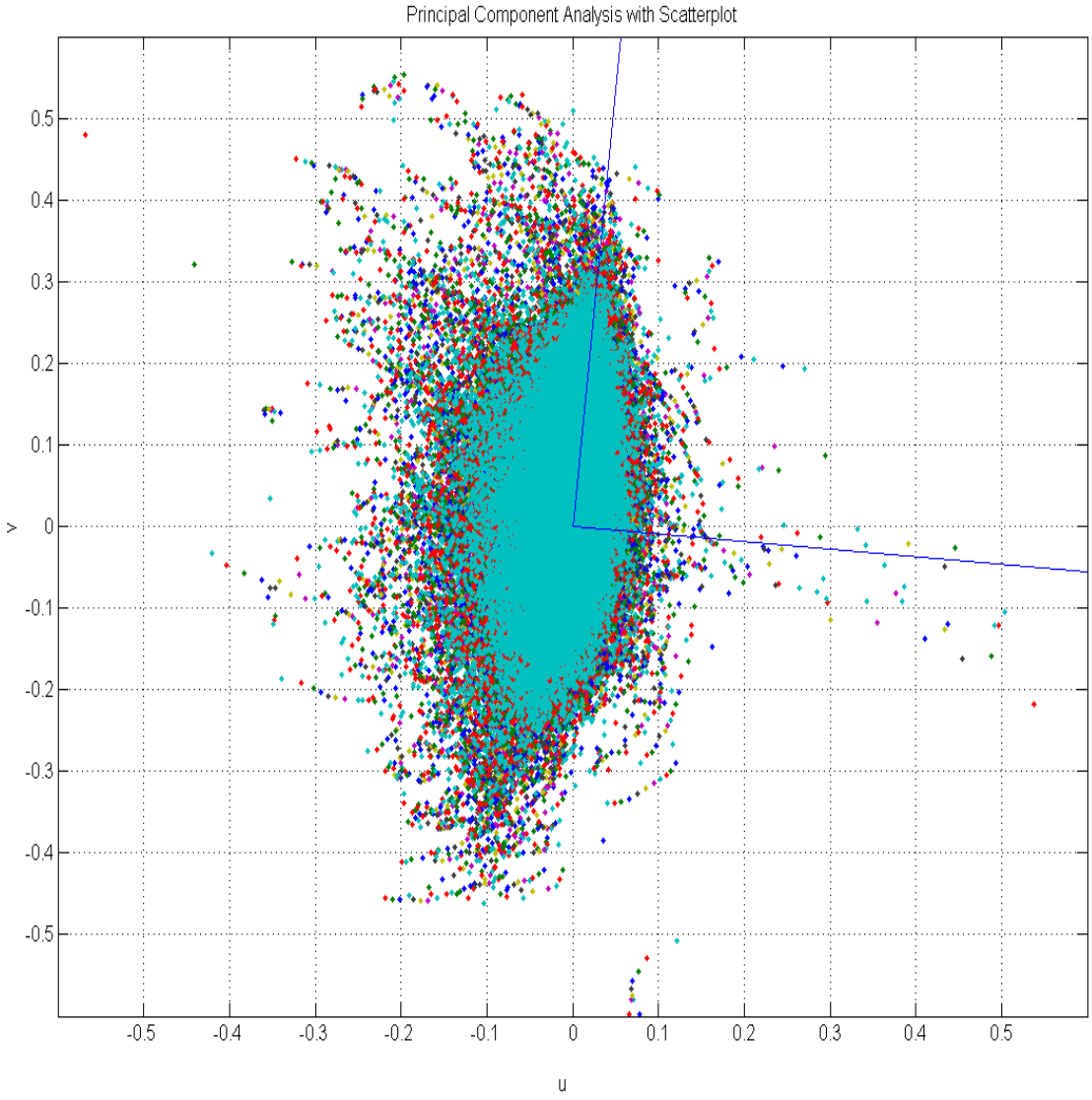

Figure 2. Principal Component Analysis of depth-averaged velocities, indicating a 10° clockwise rotation. The multiple color dots are a scatter plot of the twenty-minute mean velocities at normalized depths of z/h = 0.25 through z/h = 0.75 at 0.05 increments. The blue lines indicate the major and minor axes.

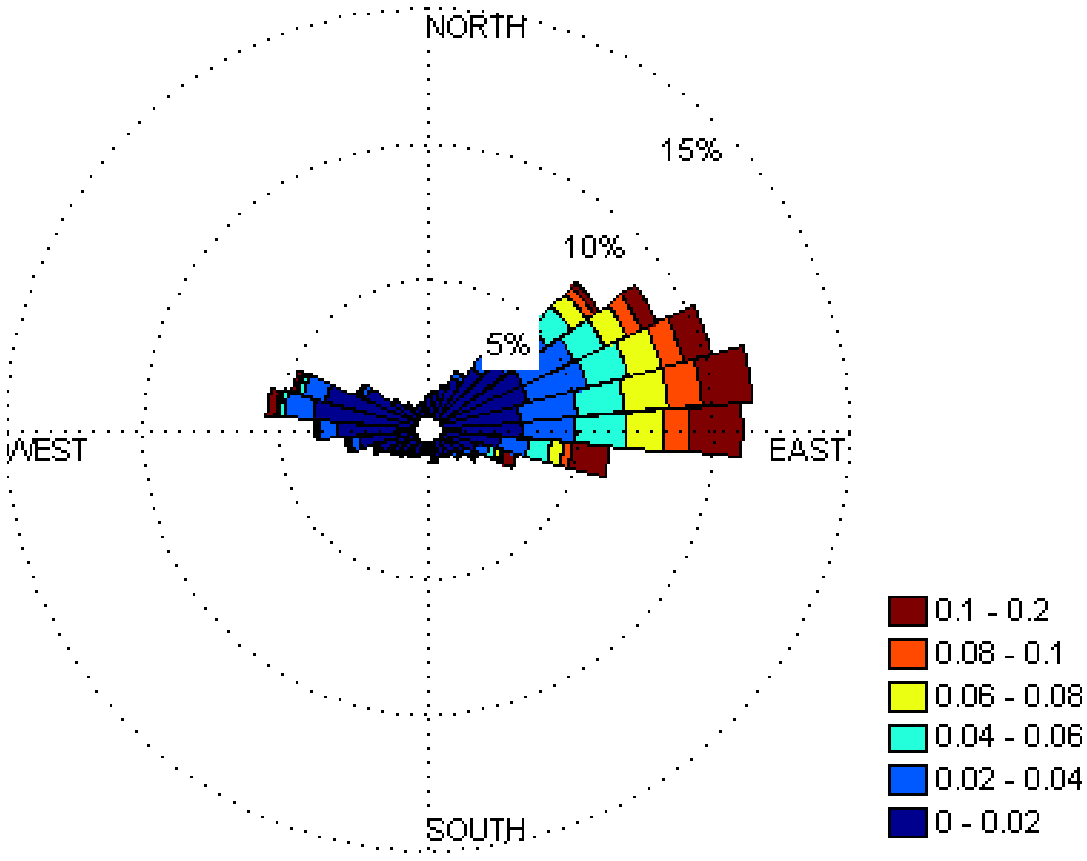

Figure 3. Wind stress rose histogram of 20-min mean of τ_s in Pa, indicating predominantly cross-shore winds.

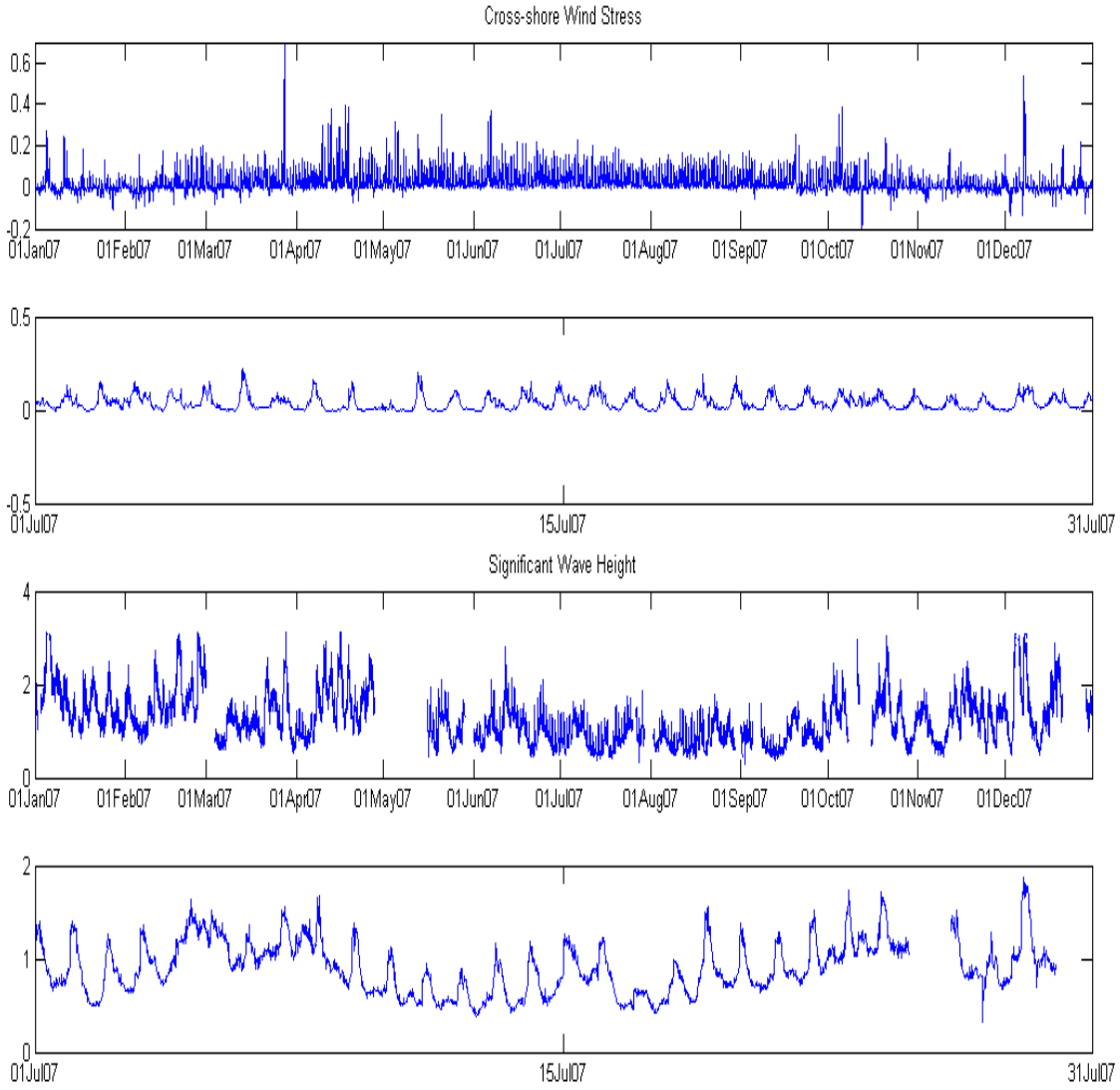

Figure 4. a.) Twenty-minute mean of τ_s for 2007 b.) Twenty-minute mean of τ_s for July 2007 c.) Twenty-minute mean of H_{sig} for 2007 d.) Twenty-minute mean of H_{sig} for July 2007

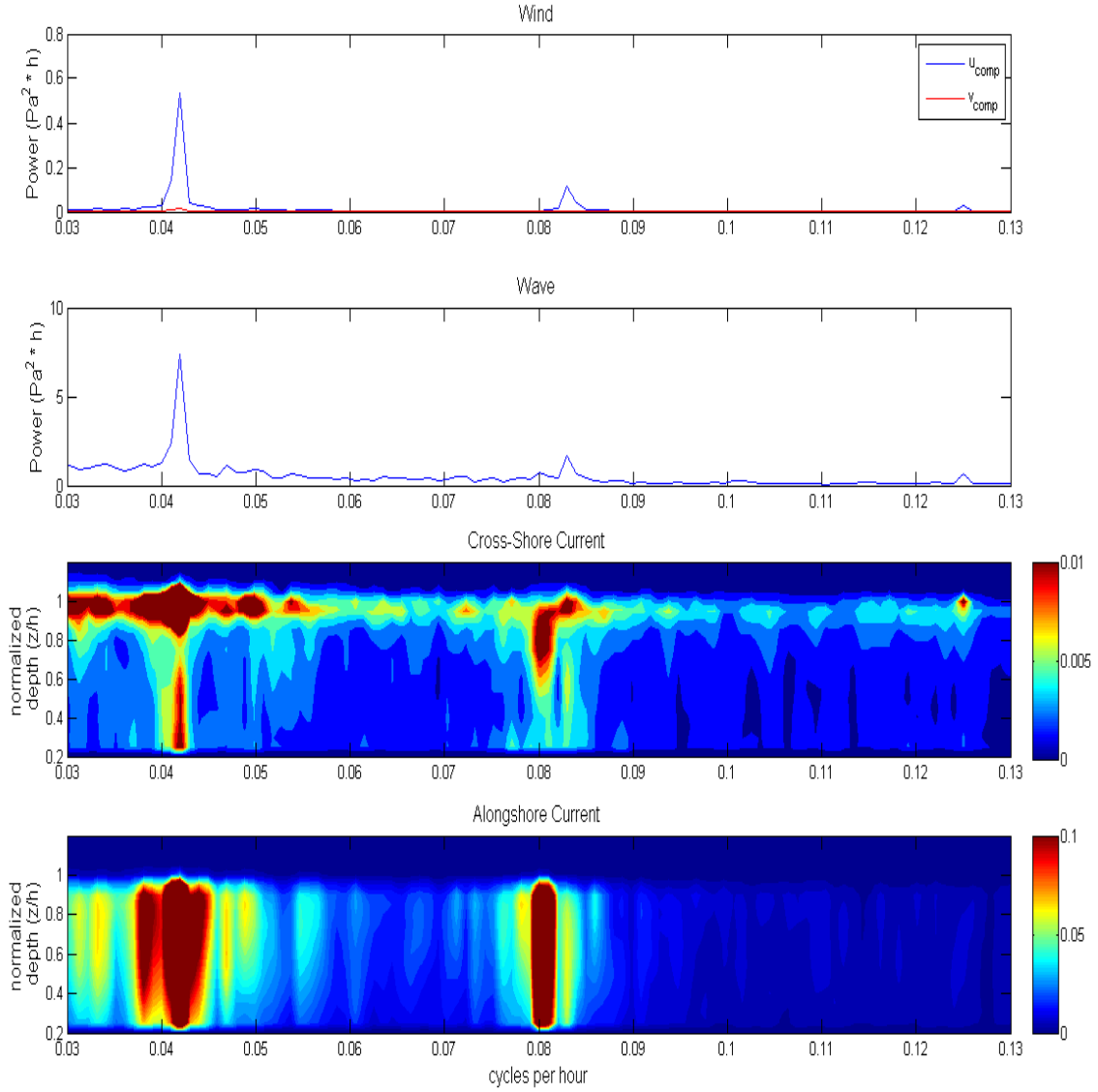

Figure 5. a.) Spectral analysis of the cross (along) - shore winds in blue (red) . b.) Spectral analysis of significant wave height. c.): Spectral analysis of the cross-shore vertical current profile. d.) Spectral analysis of the alongshore vertical current profile. Calculated on a 2 year record with 20 minute averaged signal. Spectra has 102 DOF and Δf = 0.003 cpd.

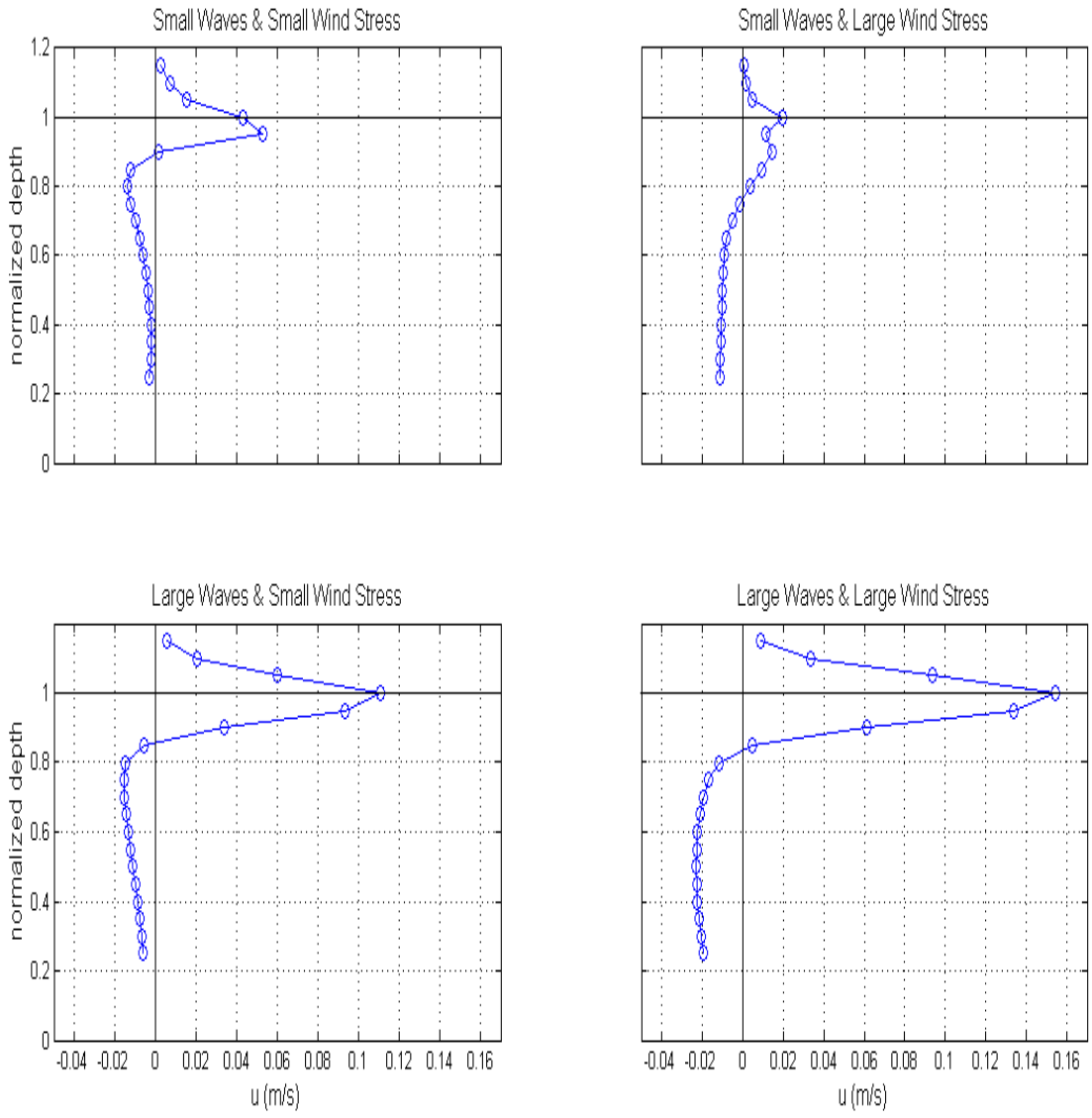

Figure 6. Hourly means of cross-shore velocity in blue circles as a function of normalized ADCP bin depth. a) when waves are small (< 0.7m) and cross-shore wind stress is small (< 0.05 Pa), b) when waves are small (< 0.7m) and cross-shore wind stress is large(> 0.1Pa), c) when waves are large (> 1.7m) and cross-shore wind stress is small (< 0.05 Pa), and d) when waves are large (> 1.7m) and cross-shore wind stress is large (>0.1Pa). The numbers in the bottom right corner of each plot represent the number of occurrences of each.

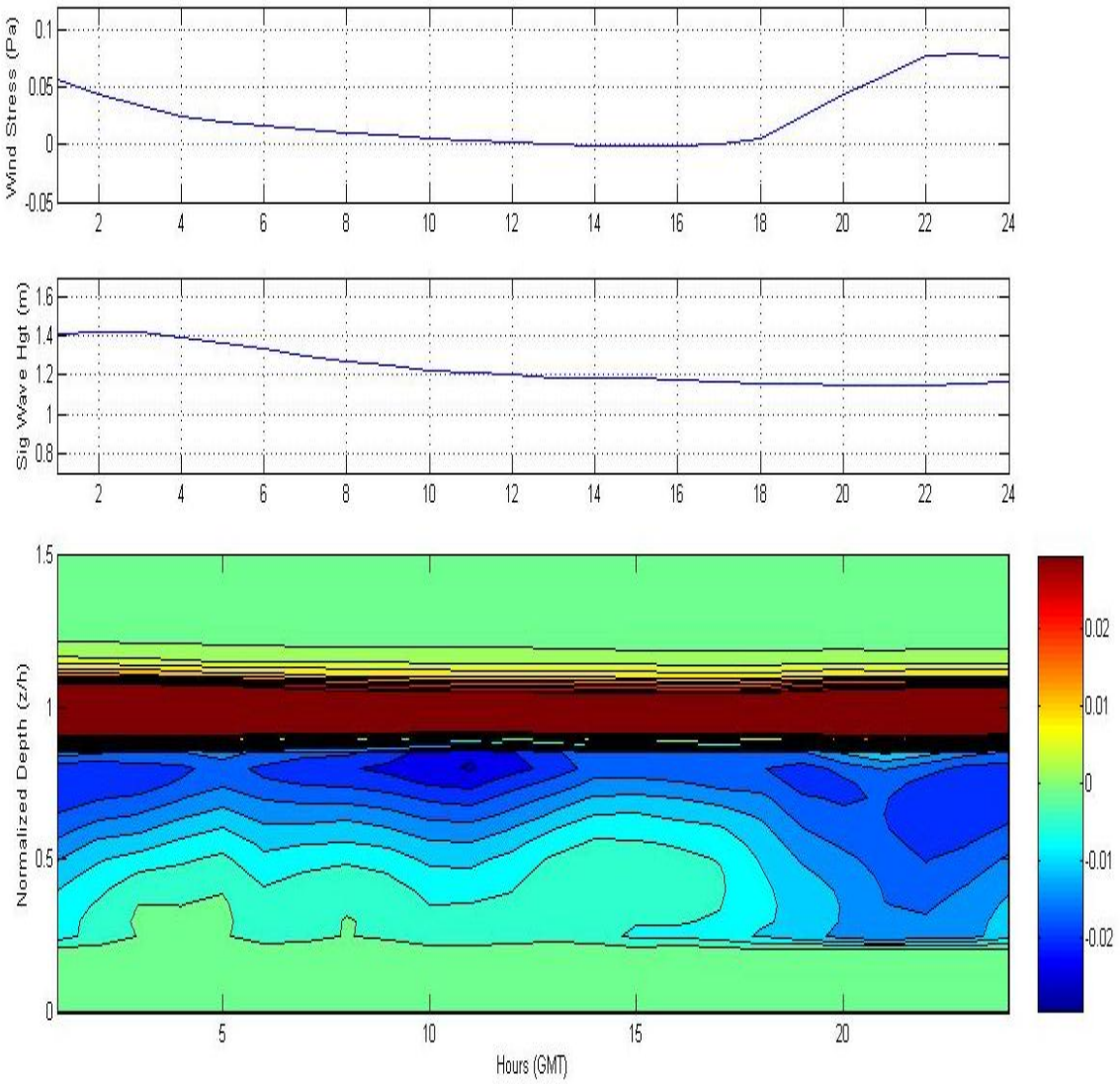

Figure 7. a.) Hourly mean of cross-shore wind stress in Pa. b.) Hourly mean of significant wave height, H_{sig} , in m. c.) Vertical profile of cross-shore current as a function of depth.

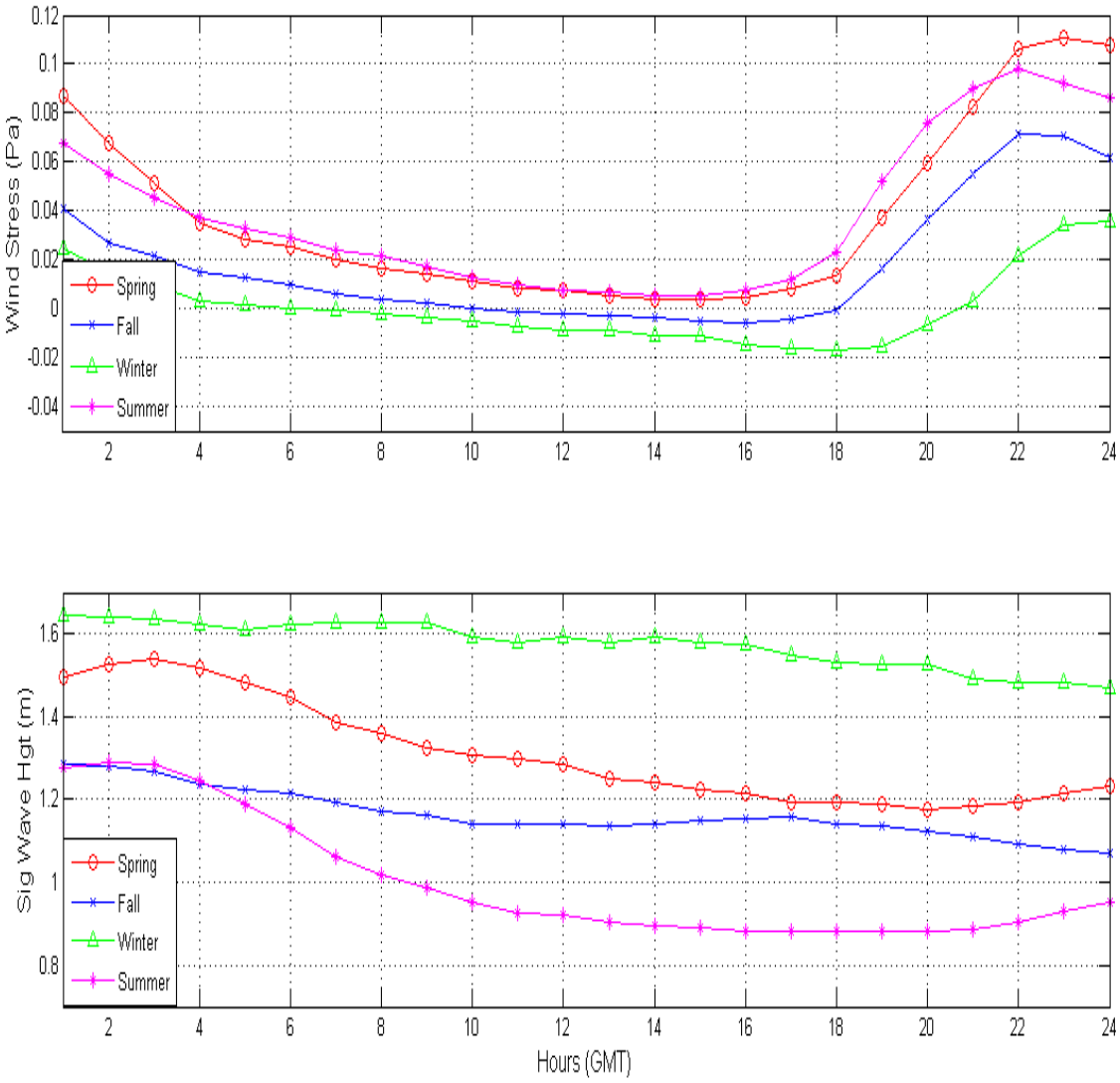

Figure 8. Seasonal Variability: Top panel) Spring (Mar/Apr/May), Top Left panel: Hourly mean of cross-shore wind stress in Pa. Spring (Mar-May) in red circles, Summer (Jun-Aug) in magenta stars, Fall (Sep-Nov) in blue balls, and Winter (Dec-Feb) green triangles. Bottom panel: Hourly mean of Significant wave height H_{sig} in m. Spring (Mar-May) in red circles, Summer (Jun-Aug) in magenta stars, Fall (Sep-Nov) in blue balls, and Winter (Dec-Feb) green triangles.

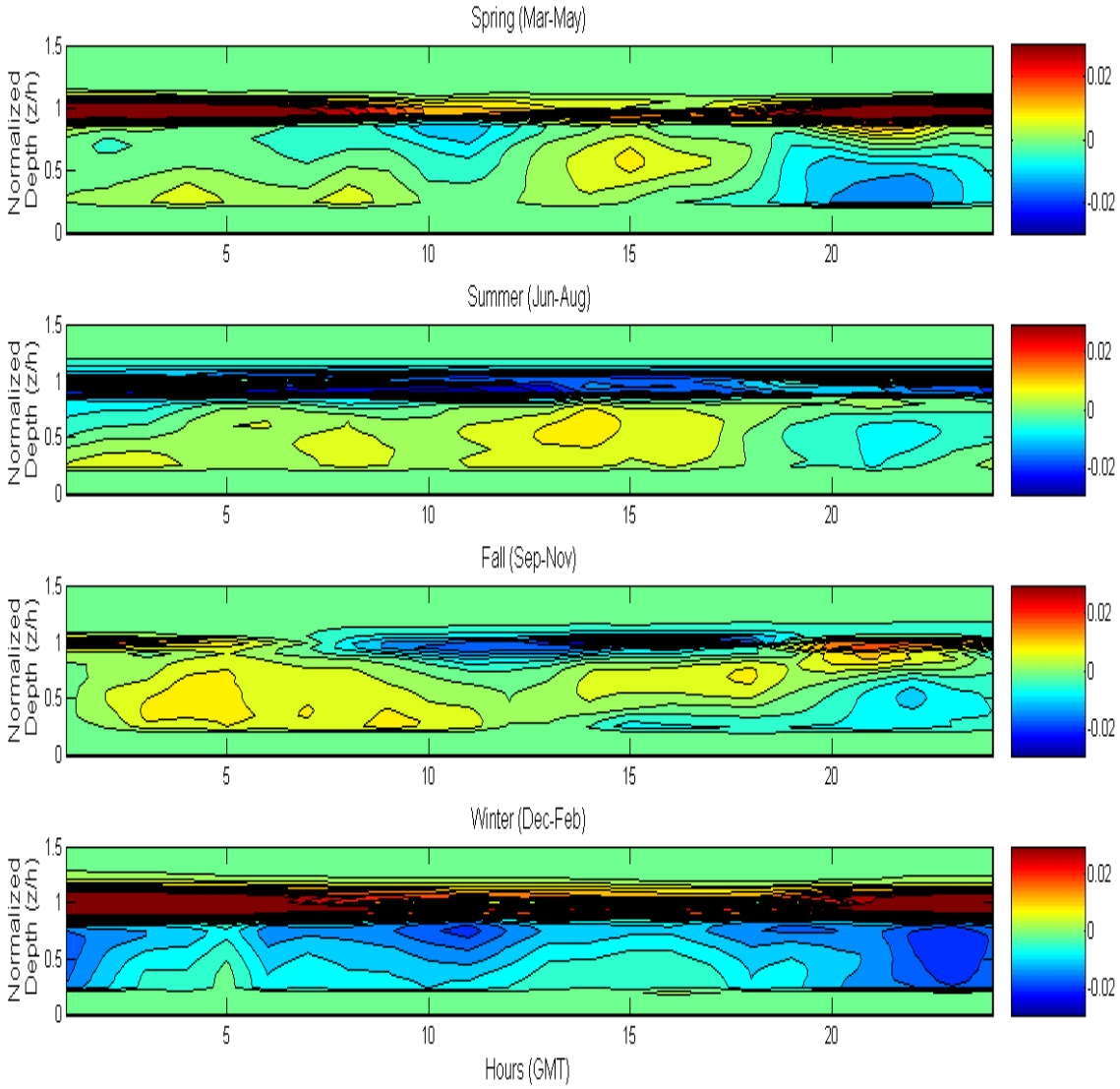

Figure 9. a.) Vertical profile of cross-shore current as a function of depth for Spring (Mar-May). b) same as for a. but for Summer (Jun-Aug). c) for Fall (Sep-Nov). d) for Winter (Dec-Feb). The current data were high-pass filtered (cutoff of 25hr).

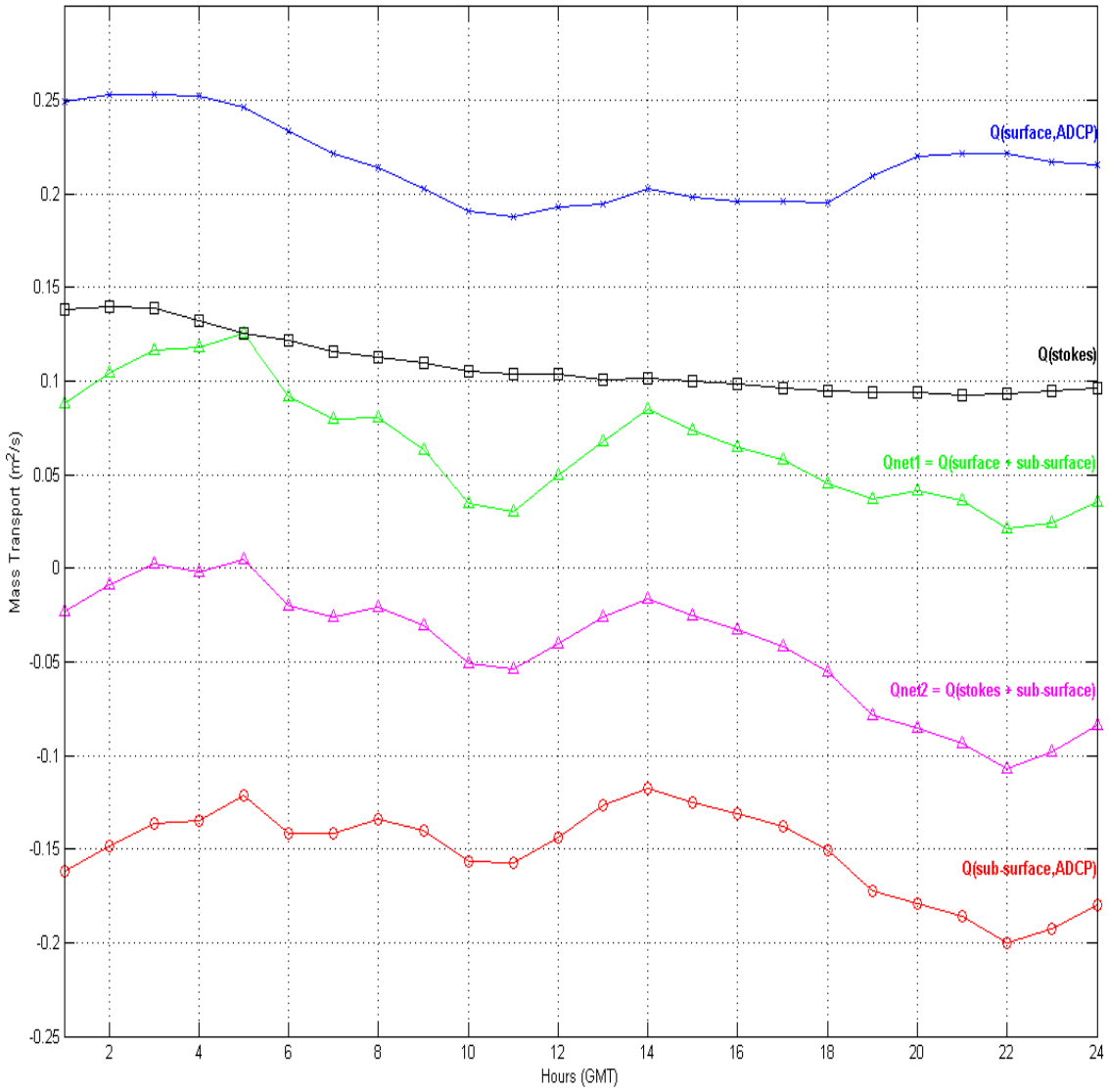

Figure 10. Mass transport: $Q_{surface,ADCP}$ (blue stars), Q_{stokes} (black squares) and $Q_{sub\text{-}surface,ADCP}$ (red circles). The first net transport (Q_{net1}) is the sum of $Q_{surface,ADCP}$ and $Q_{sub\text{-}surface,ADCP}$ (green triangles) and is onshore at 5.2×10^{-2} m^2/s. The second net transport (Q_{net2}) is the sum of Q_{stokes} and $Q_{sub\text{-}surface}$ (magenta triangles) and is offshore at 5.3×10^{-2} m^2/s.

z/h	Cross-shore current variability	Alongshore current variability	Cross-shore tidal variability	Alongshore tidal variability	Wind variability
1.0	23.9	28.2	15.7	10.7	56.3
0.75	59.5	30.4	8.0	23.1	
0.5	59.8	34.4	9.1	20.1	Wave variability
0.25	68.9	38.7	8.1	17.3	18.9
Depth-averaged	62	32	9	20	

Table 1. Current variability is the variance of the high pass filtered (cut off of 25 hr) velocity divided by the variance of the total velocity at the corresponding normalized depths (z/h). Tidal variability represents the variance of predicted tidal induced currents divided by the variance of the total velocity at the corresponding z/h. Wind variability is the variance of the high pass filtered (cut off of 25 hr) velocity divided by the variance of the total velocity. Wave variability represents the variance of the high pass filtered (cut off of 25 hr) wave height divided by the variance of the total wave height.

Diurnal Tidal Constituent	Frequency	SNR at z/h = 1.0	SNR at z/h = 0.75	SNR at z/h = 0.5	SNR at z/h = 0.25
O1	0.038731	3.8	2.3	2.6	4.6
P1	0.041553	12	2.6	1.1	1
S1	0.041667	150	8.5	9.8	9.8
K1	0.041781	8.4	18	12	16

Table 2. Diurnal tidal constituents (with a signal to noise ratio greater than 1.0) and their frequencies (cph). Signal to noise ratios (SNR) at the normalized depths of z/h =1.0, 0.75, 0.5 and 0.25 are calculated for each diurnal tidal constituent using the T_TIDE program.

LIST OF REFERENCES

Allen, J. S. "Models of Wind-Driven Currents on the Continental Shelf." *Annual Review of Fluid Mechanics* 12 (1980): 389–433.

Ardhuin, F., F. R. Martin-Lauzer, B. Chapron, P. Craneguy, F. Girard-Ardhuin, and T. Elfouhaily. "Waves and the air–sea momentum budget: Implications for ocean circulation modeling." *Journal of Physical Oceanography* 336 (2004): 1121–1130.

Ardhuin, F., N. Rascle, and K. A. Belibassakis. "Explicit wave averaged primitive equations using a generalized Lagrangian mean." *Ocean Modelling* 20 (2008c): 35–60.

Austin, J. A., and S. J. Lentz. "The Inner Shelf Response to Wind-Driven Upwelling and Downwelling." *Journal of Physical Oceanography* 32 (2002): 2171–2193.

Banta, R. M., L. D. Olivier, and D. H. Levinson. "Evolution of the Monterey sea-breeze layer as observed by pulsed Doppler lidar." *Journal of Atmospheric Sciences* 50 (1993): 3959–3982.

Banta, Robert M. "Sea Breezes Shallow and Deep on the California Coas." *Monthly Weather Review* 123, no. 12 (1995): 3614–3622.

Bendat, J. S., and A. G. Piersol. *Random Data, Analysis and Measurement Procedures.* New York: Wiley Interscience, 2000.

Bowen, Anthony J. "Rip Currents 1. Theoretical Investigations." *Journal of Geophysical Research-Oceans* 74, no. 23 (1969): 5467–5478.

Cox, Daniel T., and Nobuhisa Kobayashi. "Kinematic Undertow Model with Logarithmic Boundary Layer." *Journal of Waterway, Port, Coastal and Ocean Engineering* 123, no. 6 (1997): 354–360.

Csanady, G. T. "The Arrested Topographic Wave." *Journal of Physical Oceanography* 8, no. 1 (1978): 47–62.

Cudaback, Cynthia N., Libe Washburn, and Ed Dever. "Subtidal inner-shelf circulation near Point Conception, California." *Journal of Geophysical Research* 110, no. C10007 (2005): 1–12.

Dalrymple, R. A., and C. J. Lozano. "Wave-current interaction models for rip currents." *Journal of Geophysical Research* 83, no. C12 (1978): 6063–6071.

Davis, J. C. *Statistics and Data Analysis in Geology.* John Wiley and Sons, 1986.

Defant, F. "Local winds." *Compendium of Meteorology* (American Meteorological Society), 1951: 655–672.

Dever, E. P. "Wind-Forced Cross-Shelf Circulation on the Northern California Shelf." *Journal of Physical Oceanography* 27, no. 8 (1997a): 1566–1580.

Dever, E. P, C. E. Dorman, and J.L. Largier. "Surface boundary-layer variability off Northern California." *Deep Sea Research Part II* 53 (2006): 2887–2905.

Ekman, V. W. "On the influence of the earth's rotation on ocean-currents." *Arkiv for Matematik, Astronomi och Fysik* 2 (1905): 1–52.

Emery, William J., and Richard E. Thomson. *Data Analysis Methods in Physical Oceanography.* 2. Elsevier, 2001.

Falkowski, Paul G., Richard T. Barber, and Victor Smetacek. "Biogeochemical Controls and Feedbacks on Ocean Primary Production." *Science* 281 (1998): 200–206.

Fewings, Melanie, Steven J. Lentz, and Janet Fredericks. "Observations of Cross-Shelf Flow Driven by Cross-Shelf Winds on the Inner Continental Shelf." *Journal of Physical Oceanography* 38, no. 11 (2008): 2358–2378.

Haines, John W., and Asbury H. Sallenger Jr. "Vertical structure of mean cross-shore currents across a barred surf zone." *Journal of Geophysical Research* 99, no. C7 (1994): 14223–14242.

Hasselmann, K. "Wave-driven inertial oscillations." *Geophysical & Astrophysical Fluid Dynamics* 1, no. 3 (1970): 463–502.

Herbers, T. H. C., Steve Elgar, and R. T. Guza. "Infragravity-Frequency (0.005–0.05 Hz) Motions on the Shelf. Part I: Forced Waves." *Journal of Physical Oceanography* 24, no. 5 (1994): 917–927.

Inman, Douglas L., and Birchard M. Brush. "The Coastal Challenge." *Science*, 1973: 20–32.

Kirincich, A. R., J. A. Barth, B. A. Grantham, B. A. Menge, and J. Lubchenco. "Wind-driven inner-shelf circulation off central Oregon during summer." *Journal of Geophysical Research* 110, no. C10S03 (2005).

Lentz, S. J. "The surface boundary layer in coastal upwelling regions." *Journal of Physical Oceanography* 22 (1992): 1517–1539.

Lentz, Steve, R. T. Guza, S. Elgar, F. Feddersen, and T. H. C. Herbers. "Momentum balances on the North Carolina Inner Shelf." *Journal of Geophysical Research* 104, no. C8 (1999): 1–26.

Lentz, Steven J. "Current Dynamics over the Northern California Inner Shelf." *Journal of Physical Oceanography* 24, no. 12 (1994): 2461–2478.

Lentz, Steven J., Melanie Fewings, Peter Howd, Janet Fredericks, and Kent Hathaway. "Observations and a Model of Undertow over the Inner Continental Shelf." *Journal of Physical Oceanography* 38, no. 11 (2008): 2341–2357.

Lentz, Steven J. "The Influence of Stratification on the Wind-Driven Cross-Shelf Circulation over the North Carolina Shelf." *Journal of Physical Oceanography* 31, no. 9 (2001): 2749–2760.

Longuet-Higgins, M. S. "Mass Transport in Water Waves ." *Philosophical Transactions of the Royal Society of London. Series A, Mathematical and Physical Sciences* 245, no. 903 (1953): 535–581.

Madsen, Ole Secher. "Mass Transport in Deep-Water Waves." *Journal of Physical Oceanography* 8, no. 6 (1978): 1009–1015 .

Massel, Stanislaw R. *Ocean Surface Waves: Their Physics and Prediction.* World Scientific, 1996.

Militello, Adele, and Nicholas C Kraus. "Generation of Harmonics by Sea Breeze in Nontidal Water Bodies." *Journal of Physical Oceanography* 31, no. 6 (2001): 1639–1647.

Monosmith, S. G., E. A. Cowen, H. M. Nepf, J. Magnaudet, and L. Thais. "Laboratory observations of mean flows under surface gravity waves." *Journal of Fluid Mechanics* 573 (2007): 131–147.

Ogasawara, T., and T. Yasuda. "Mass flux and vertical distribution of currents caused by strong winds in a wave tank." *Journal of Physical Oceanography* 34, no. 12 (2004): 2712–2720.

Pawlowicz, R., R. Beardsley, and S. Lentz. "Classical tidal harmonic analysis including error estimates in MATLAB using T_TIDE." *Computers and Geosciences* 28 (2002): 929–937.

Petruncio, Emil T., Leslie K. Rosenfeld, and Jeffrey D. Paduan. "Observations of the Internal Tide in Monterey Canyon." *Journal of Physical Oceanography* 28, no. 10 (1998): 1873–1903.

Pilskaln, Cynthia H., Jennifer B. Paduan, Francisco P. Chavez, Roger Y. Anderson, and William M. Berelson. "Carbon export and regeneration in the coastal upwelling system of Monterey Bay, central California." *Journal of Marine Research* 54, no. 6 (1996): 1149–1178.

Putrevu, Uday, and Ib A. Svendsen. "Vertical Structure of the Undertow Outside the Surf Zone." *Journal of Geophysical Research-Oceans* 22, no. 98(C12) (1993): 707–22.

Rascle, N., F. Ardhuin, P. Queffeulou, and D. Croiz´e-Fillon. "A global wave parameter database for geophysical applications. Part 1: wave-current-turbulence interaction parameters for the open ocean based on traditional parameterizations." *Ocean Modelling* 25 (2008): 154–171.

Reniers, A. J. H. M., E. B. Thornton, T. P. Stanton, and J. A. Roelvink. "Vertical flow structure during Sandy Duck: observations and modeling." *Coastal Engineering* 51, no. 3 (2004): 237–260.

Rosenfeld, L. K., F. Schwing, N. Garfield, and D. E. Tracy. "Bifurcated flow from an upwelling center: A cold water source for Monterey Bay." *Continental Shelf Research* 14 (1994): 931–964.

Rosenfeld, Leslie, Igor Shulman, Michael Cook, Jeff Paduan, and Lev Shulman. "Methodology for a regional tidal model evaluation, with application to central California." *Deep Sea Research Part II*, Article in Press.

Shepard, F. P., K. O. Emery, and E. C. La Fond. "Rip currents: A process of geological importance." *Journal of Geology* 49 (1941): 337– 369.

Simpson, John E. *Sea Breeze and Local Winds.* Cambridge: Cambridge University Press, 1994.

Smith, Jerome A. "Wave–Current Interactions in Finite Depth." *Journal of Physical Oceanography* 36 (2006): 1403–1419.

Smith, Stuart D. "Coefficients for sea surface wind stress." *Journal of Geophysical Research* 93, no. C12 (1988): 15467–15472.

Stokes, G. G. "On the theory of oscillatory waves." *Transactions of the Cambridge Philosophical Society* 8 (1847): 441–455.

Sverdrup, HU. "On the process of upwelling." *Journal of Marine Research* 1 (1938): 155–164.

Thornton, E. B., and R. T. Guza. "Transformation of wave height distribution." *Journal of Geophysical Research* 88 (1983): 5925–5938.

Tilburg, C. E. "Across-shelf transport on a continental shelf: Do across-shelf winds matter?" *Journal of Physical Oceanography* 33 (2003): 2675–2688.

Ting, F. C. K., and J.T. Kirby. "Observation of undertow and turbulence in a laboratory surf zone." *Coastal Engineering* 24 (1994): 51–80.

Trenberth, Keven E. "What are the Seasons?" *Bulletin of the American Meteorological Society* 64, no. 11 (1983): 1276–1282.

Ursell, F. "Surface waves on deep water in the presence of a submerged circular cylinder, I,II." *Proceedings of the Cambridge Philosophical Society* 46 (1950): 141–158.

Weatherly, Georges L, and Paul J. Martin. "On the Structure and Dynamics of the Oceanic Bottom Boundary Layer." *Journal of Physical Oceanography* 8, no. 4 (1978): 557–570.

Woodson, C.B, et al. "Local diurnal upwelling driven by sea breezes in northern Monterey Bay." *Continental Shelf Research* 27, no. 18 (2007): 2289–2302.

Wu, Jin. "Sea-Surface Drift Currents Induced by Wind and Waves." *Journal of Physical Oceanography* 13, no. 8 (1983): 1441–1451.

Xu, Zhigang, and A. J. Bowen. "Wave- and Wind-Driven Flow in Water of Finite Depth." *Journal of Physical Oceanography* 24, no. 9 (1994): 1850–1866.

THIS PAGE INTENTIONALLY LEFT BLANK

INITIAL DISTRIBUTION LIST

1. Defense Technical Information Center
   Ft. Belvoir, Virginia

2. Dudley Knox Library
   Naval Postgraduate School
   Monterey, California

3. Professor Jamie MacMahan
   Naval Postgraduate School
   Monterey, California

4. Lt. Col. Karl Pfeiffer
   Naval Postgraduate School
   Monterey, California

5. Professor Jeffrey Paduan
   Naval Postgraduate School
   Monterey, California

6. Professor Phillip Durkee
   Naval Postgraduate School
   Monterey, California